Chapter 6

Experimental Study into UVAMQL Grinding of AISI D2 Tool Steel with an Alumina Wheel Using Eco-friendly Cutting Fluids

6 Introduction

Due to increased environmental regulations and intensive market competition, the optimisation of machining operations, a crucial component of the manufacturing cycle, is currently essential. The use of ultrasonic vibration assisted grinding (UVAG) to improve grinding performance has been established in previous chapters. These improvements can be attributed to the change in cutting process dynamics enabled by UVAG. Conversely, applying a minimum quantity lubrication (MQL) technique has been shown to be beneficial in improving the lubrication characteristics of the cutting fluid while simultaneously minimising its consumption and mitigating its environmental impact. However, only a limited number of studies have been conducted on the synergistic application of both techniques. Their individual influence mechanisms do not appear to interfere with each other. Consequently, there is potential for enhancing the grinding process by combining these techniques, commonly named ultrasonic vibration assisted minimum quantity lubrication (UVAMQL) grinding.

This chapter endeavour seeks to meticulously evaluate the effectiveness of UVAMQL grinding on difficult-to-machine materials such as AISI D2 tool steel using four sustainable cutting fluids, namely, soybean oil (SO), soybean oil-deionized water (SO + DW) emulsion, and aluminium oxide nanofluids (Al_2O_3 NFs) with two weight percentages (wt%) of 0.5 and 1.0 wt% in an effort to simultaneously maximise production quality in terms of the grinding force, surface roughness, surface functional parameters, surface topography, chip morphology, and grinding temperature and reduce environmental

concerns associated with the grinding process. Besides, the existing body of literature referenced in Chapter 2 has indicated that vegetable oils possess desirable attributes such as low global warming potential and friction reduction capabilities, rendering them highly suitable for replacing mineral-based cutting fluids in grinding processes. The inclusion of vegetable oil in deionized water as a biodegradable emulsion for UVAMQL grinding has been selected due to its ability to form a densely packed and robust lubricating film on the work surface. Furthermore, the utilization of nanofluids as cutting fluids during UVAMQL grinding of AISI D2 tool steel has yielded improvements in heat transfer phenomena and facilitated the development of a metallic lubricating layer in the grinding zone, which exhibits anti-friction and anti-wear properties. Different weight concentrations of Al_2O_3 nanoparticles have been chosen for comparison purposes to prepare the Al_2O_3 NFs for UVAMQL grinding.

The assessment of prepared cutting fluids' quality and stability was conducted by examining their pH values and micrographs using the sedimentation method. Furthermore, the properties of the cutting fluids were evaluated through the measurement of thermal conductivity, viscosity, surface tension, and contact angles with the work material.

6.1 Experimental procedure

6.1.1 Work material, grinding wheel, and UVAMQL grinding

In this study, the work material was AISI D2 tool steel (58 ± 2 HRC), with sample dimensions of $70^{L}\times10^{T}\times15^{W}$ mm. Details of the work material used, chemical composition, and heat treatment procedure were detailed in Chapter 3, section 3. The experiments were carried out using a precision surface grinding machine with white alumina grinding wheel. Details about the abrasive wheel designation and dressing setting are detailed in Chapter 3, section 3.1. The details about the indigenously developed UVAMQL grinding setup were

Table 6.1 UVAMQL grinding experimental settings

Parameters	Conditions
Grinding mode	Plunge surface grinding
Wheel specifications	AA60K5V6
Wheel dimensions	250 ×76.5 ×25 mm
Wheel speed (V_c)	39.42 m/s
Worktable feed rate (V_w)	9 mm/min
Downfeed (a_p)	40 µm
Vibration frequency for horn (f_{ug})	21 kHz
Vibration amplitude for horn (A_{ug})	10 µm
Nozzle diameter	ϕ 1 mm
Fluid reservoir capacity	250 ml
Flow rate (Q): vegetable oil	200 ml/h
Oil-water emulsion and nanofluids	150 ml/h
Air Pressure (P)	4 bar
Stand-off distance (Z): vegetable oil	50 mm
Oil-water emulsion and nanofluids	40 mm
MQL Nozzle angle (α)	12°

discussed in Chapter 3, section 3.4. The thermo-mechanical properties of AISI D2 tool steel are mentioned in Chapter 4 in Table 4.5. The UVAMQL grinding experimental

specifications illustrated in Table 6.1 were adequately taken based on the preliminary experiments.

6.1.2 Procedure for characterisation of cutting fluids and grindability

There were two categories of experiments: non-machining experiments and grinding experiments. In the category of non-machining experiments, pH test, stability test, density, thermal conductivity, viscosity, contact angle, and surface tension were selected as the output responses. All non-machining tests were conducted at ambient temperature (25 °C) to study the lubricating performance of different cutting fluids before UVAMQL grinding. In the grinding experiment category, grinding force, surface roughness, surface functional parameters, surface topography, microchip morphology, and grinding temperature have been considered the output responses. Chapter 3, Sections 3.6 and 3.7, discusses the detailed procedures for the above characterisations.

6.1.3 Selection, preparation, and stability of sustainable cutting fluids

For UVAMQL grinding, choosing the right cutting fluids is crucial since they determine the lubricating qualities and heat transfer from the grinding region. Therefore, four sustainable cutting fluids, namely, soybean oil (SO), soybean oil-deionized water (SO + DW) emulsion, and aluminium oxide nanofluids (Al_2O_3 NFs) with two weight percentages (wt%) of 0.5 and 1.0 wt% were chosen as UVAMQL cutting fluids are shown in Figure 6.1 (a). The QUALIKEMS Fine Chem Pvt. Ltd. provided soyabean oil along with a lab report. It contains a high concentration of polyunsaturated fatty acids (61%), as well as linoleic acid (52.4%), monounsaturated fatty acids (24%), oleic acid (23%), and linolenic acid (10.6%), with polarity head groups (refer to Figure 6.1 2(b)), which improves its anti-friction and anti-wear characteristics [107]. The essential physical properties of soybean oil are shown in Table 6.2. Due to relatively low volatility, deionized water is needed to boost

cooling efficiency in the grinding zone. In the current study, SO+DW emulsion cooling performance was enhanced by adding a small amount (0.5 and 1 wt%) of Al_2O_3 nanoparticles. The Otto Chemie Pvt. Ltd. provided the Al_2O_3 nanoparticles (NPs) with 99% purity, and the physical properties of Al_2O_3 NPs present in Table 6.3. The X-ray powder diffraction technique/XRD (maker: Rigaku, Model: Ultima-IV, H-12) was used with a scan speed of 0.02°/sec to identify the different phases and crystallinity of NPs. The Cu Kα (λ = 1.5604 Å) radiation was employed on Al_2O_3 NPs with an operating voltage of 35 kV and a current of 25 mA. The XRD data was collected in the 9° to 90° range and intensity vs 2θ graph of Al_2O_3 NPs is shown in Figure 6.2 (a).

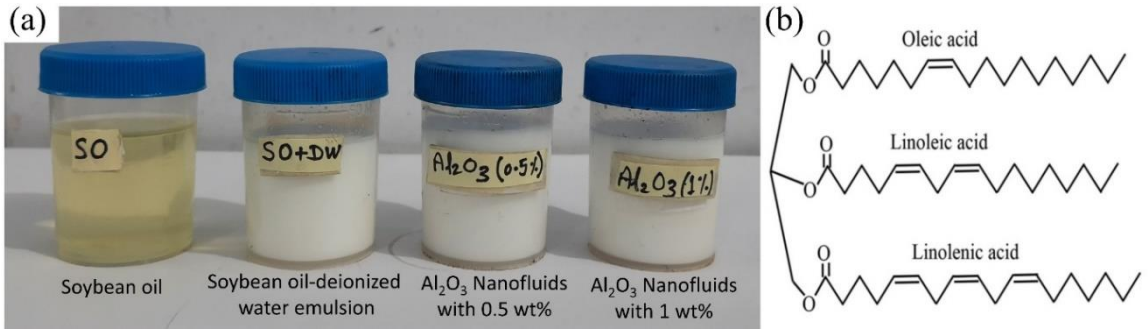

Figure 6.1 (a) Prepared eco-friendly cutting fluids used in UVAMQL grinding, (b) Molecular structure of soybean oils

Table 6.2 Physical properties of SO at ambient temperature

Density (kg/m^3)	Viscosity (centipoise)	Pour point (˚C)	Flash point (˚C)
923	42	-24	240

Table 6.3 Physical properties of Al_2O_3 nanoparticles

Actual particle size (nm)	Molecular weight (g/mol.)	Specific surface area (m^2/g)	Thermal conductivity (W/m.K)	Density (kg/m^3)
50	101.96	125	30	3880

The Al_2O_3 NPs' XRD peaks diffractograms were compared to a gamma-Al_2O_3 NPs with X'Pert Highscore reference number 98-003-0267. In accordance with the standard dataset,

the diffractograms of Al_2O_3 NPs exhibited five different reflections at 2θ angle = 19.11° (002), 39.47° (111), 45.89° (002), 56.94° (022), and 84.97° (222). Using a transmission electron microscope (maker: FEI Company of USA, Model: Tecnai G2-20 TWIN), the size of the Al_2O_3 nanoparticles and surface morphology were evaluated. Figure 6.2 (b) shows the nearly spherical appearance of Al_2O_3 nanoparticles.

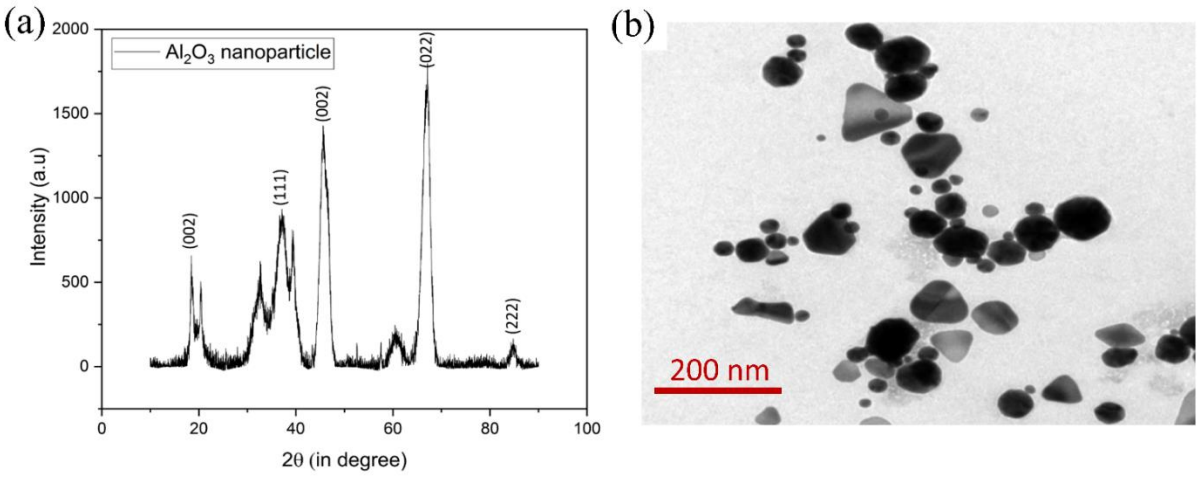

Figure 6.2 (a) XRD analysis of Al_2O_3 powder, (b) TEM image of Al_2O_3 powder

TWEEN-20 is used in the present research as an emulsifying agent to prepare stable soybean oil emulsions in deionized water. By stirring with a magnetic stirrer for 60 minutes, the emulsifying agent (0.5mL) was dissolved in soybean oil (10mL). Then, this mixture was poured into 200mL of deionized water and stirred for 60 minutes using a magnetic stirrer. It was then sonicated for another 120 minutes using an ultrasonic probe sonicator. Similar procedures have been followed to mix the Al_2O_3 NPs in the SO+DW emulsion. A little amount of sodium laurilsulfate surfactant (5 wt% of NPs) is added to the Al_2O_3 NFs to increase the stability of the Al_2O_3 NPs in the SO+DW emulsion. In order to create a stable solution of Al_2O_3 NPs in SO+DW emulsion, 240 repetitions of a 30-second on and 7-second off cycle were performed at ambient temperature in a probe sonicator. Figure 6.3 demonstrates the steps involved in developing a sustainable emulsion and Al_2O_3

nanofluids. The pH value of nanofluids is measured using a digital pH metre (maker: ISO Tech System, Model-ITS 201) to determine their stability, as shown in Figure 6.4 (a-b). All tests were conducted three times to determine the average value of the test data. In this experiment, the isoelectric point (IEP) pH of Al_2O_3 NPs (9.6) was compared to the average pH values of 0.5 and 1 wt% of Al_2O_3 NFs (i.e., 7.5 and 8.7, respectively).

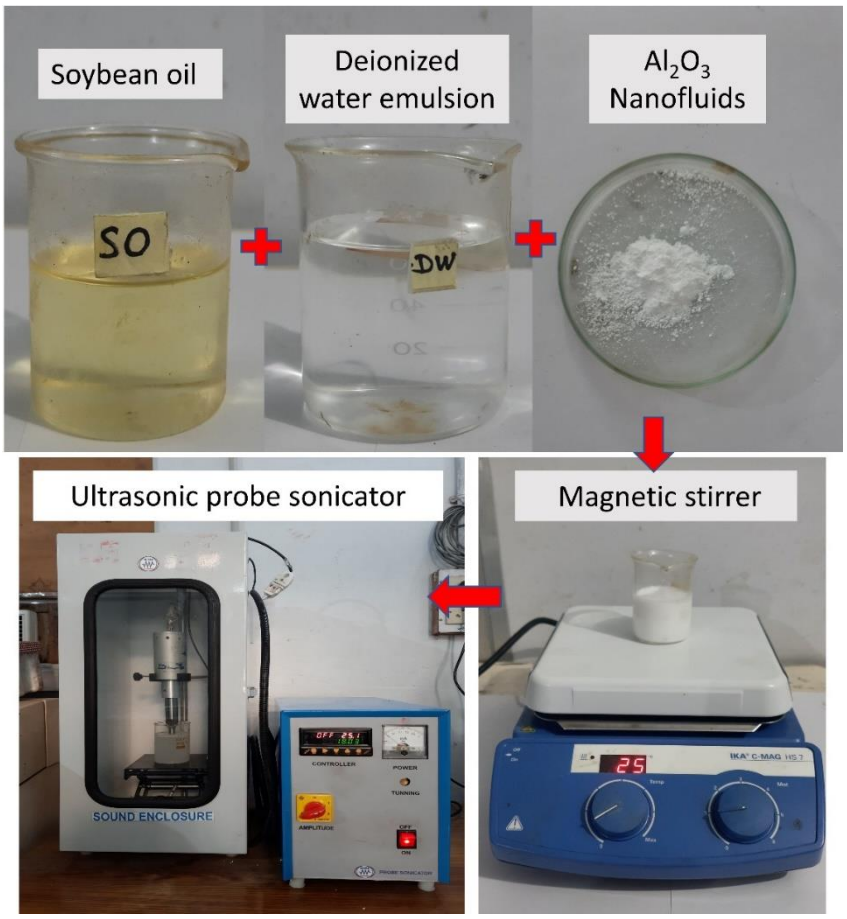

Figure 6.3 Al_2O_3 NFs preparation stages

Based on the Derjaguin–Landau–Verwey–Overbeek (DLVO) hypothesis [275], NFs are naturally unstable when the pH is the same or near the IEP, forming clusters and precipitation. Because of the small particle-particle repulsive force or surface energy of NPs, as a result, reduced stability, and high aggregated lubricant of Al_2O_3 NFs (1 wt%), the

pH value differed by one. Furthermore, a twofold difference in the pH of Al_2O_3 NFs (0.5 wt%) and the IEP of Al_2O_3 NPs was found; the suspension particles became more stable.

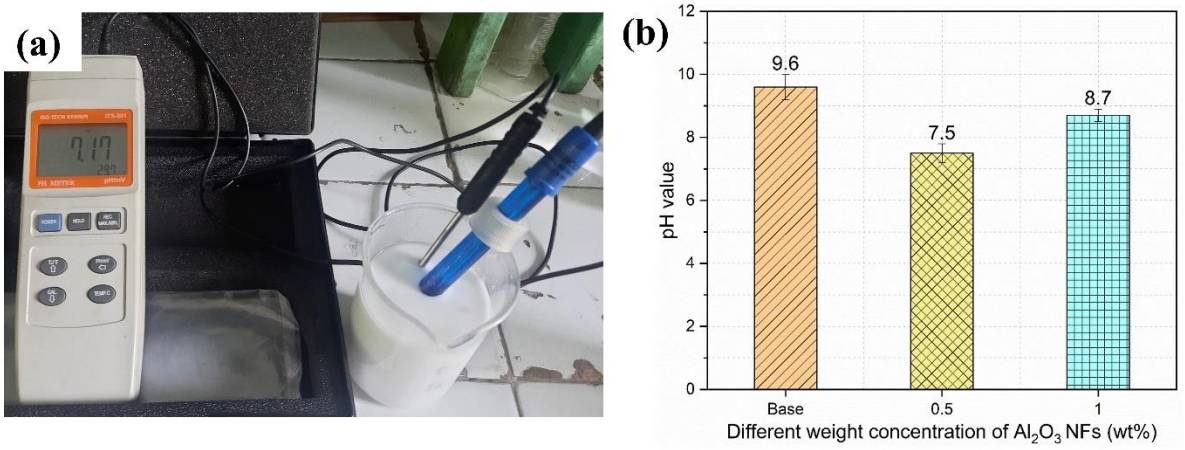

Figure 6.4 (a) Digital pH meter system, (b) pH values of different concentrated Al_2O_3 NFs

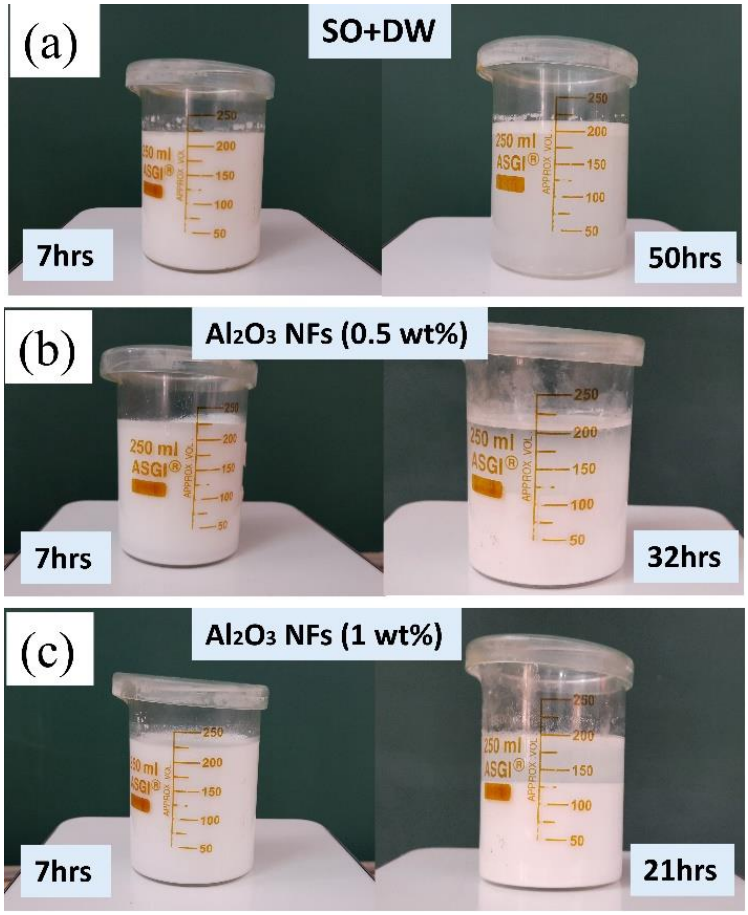

Figure 6.5 Stability of different concentrated Al_2O_3 nanofluids

Utilizing the sedimentation technique, the dispersal of the SO+DW emulsions and Al_2O_3 NFs was evaluated. A glass beaker was filled with 200 mL of emulsions, and emulsions were allowed to settle for many hours. Figure 6.5 (a-c) illustrates photographs of synthesized SO+DW emulsion and Al_2O_3 NFs over 7–50 hours. Figure 6.5 (a) shows how stable the SO+DW emulsion is over a long period. The possible explanations are that the emulsifying agent used atoms of soyabean oil to make self-assembling molecular clusters, which were then taken up by the hydrogen phase to make the SO and DW interfaces. The Al_2O_3 NFs (1 wt%) were stable for 21 hours; over the next 3 hours, the slow settlement of NPs in the emulsion due to gravity and the high proportion of Al_2O_3 NPs caused NPs to stick together in the emulsion. When NPs stick together, they change their Brownian motion, making them even less stable.

6.1.4 Density of cutting fluid

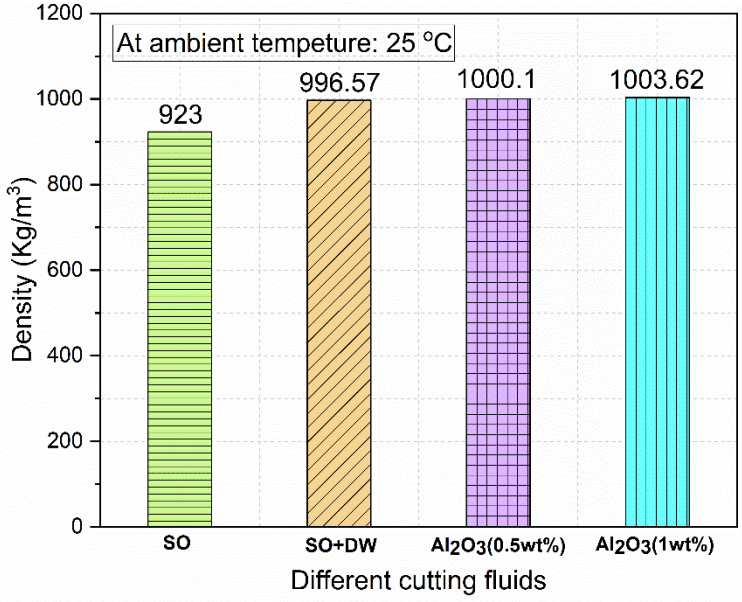

Figure 6.6 Variation in density of different cutting fluids

Density plays a significant role in determining the fluid's behaviour and properties. The density of vegetable oil-based deionized water emulsion is lower than that of pure water due to the presence of oil droplets in the emulsion. On the other hand, the density of

nanofluid is higher than that of the base fluid due to the addition of nanoparticles, as shown in Figure 6.6. The density of nanofluid increases with increasing nanoparticle concentration and decreasing temperature [276]. The presence of emulsifiers can also affect the density of the mixture as they can increase the stability of the emulsion and alter its physical properties. Therefore, lubricants with higher densities can provide better cooling and lubrication, resulting in improved machining performance.

6.1.5 Thermal conductivity of cutting fluid

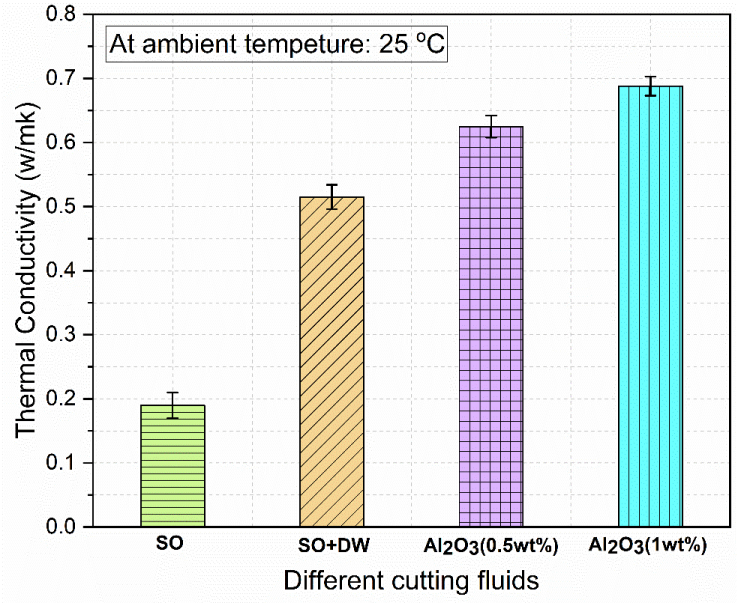

Figure 6.7 Thermal conductivity of different cutting fluids

The thermal conductivity of a working fluid has a significant impact on how well it transfers heat because higher thermal conductivity encourages faster heat transfer. Figure 6.7 illustrates the measured thermal conductivity value obtained from the experiment. The addition of deionized water to base fluid such as vegetable oil leads to an increase in thermal conductivity, as water contains a higher thermal conductivity compared to oil. Additionally, adding NPs to the emulsion can further enhance the thermal conductivity of the nanofluid, as NPs can act as heat conductors and increase the effective thermal conductivity of the mixture. The thermal conductivity of the emulsion and nanofluid is influenced by various

factors such as nanoparticle concentration, temperature, and particle size distribution. Therefore, the thermo-physical characteristics of vegetable oil-based emulsions and NFs need to be carefully characterized and optimized to ensure their effective use in heat transfer applications. Similarly, Kong and Lee [277] concluded that Al_2O_3 NFs exhibit enhanced thermal conductivity compared to their base fluids (water), which can be ascribed to the high thermal conductivity of the NPs and their ability to form a stable suspension in the base fluid. It was found that higher thermal conductivity can effectively enhance the performance of heat transfer.

6.1.6 Viscosity of cutting fluid

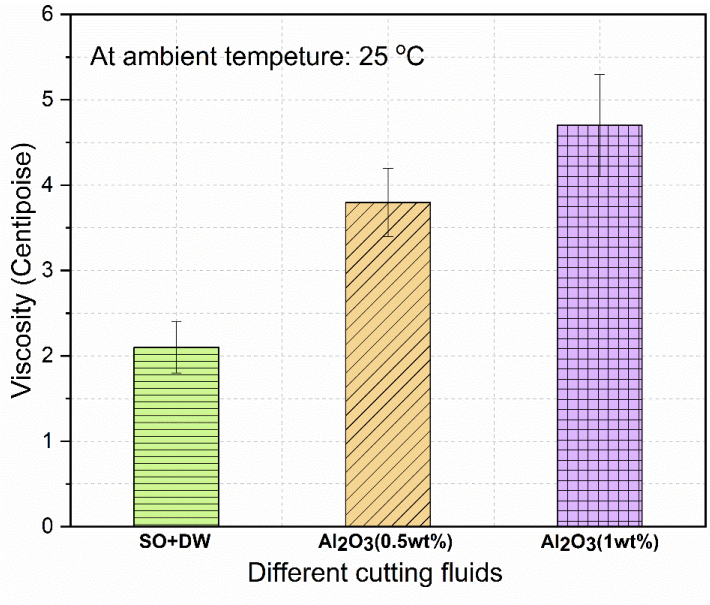

Figure 6.8 Viscosity of different UVAMQL cutting fluids

Viscosity is a measure of the internal friction of a fluid, and it is directly related to the fluid's flow rate. The higher the viscosity of the emulsion or nanofluid, the more difficult it is for the particles to move freely, which affects the suspension's stability and heat transfer. Therefore, the viscosity of the base fluid, emulsion and nanofluids play an essential role in their physical behaviour and performance in various applications, such as suspension stability, heat transfer, lubrication, and energy storage. By studying the role of viscosity in

these fluids, researchers can develop strategies to enhance their stability and heat transfer efficiency, leading to improved performance and sustainability. The viscosity of the lubricants was measured using a viscometer with an accuracy of ±1%. Figure 6.8 reveals the variation in the viscosity of NFs with different wt.% concentrations of Al_2O_3 NPs. From Table 6.2, it was noticed that SO has maximum viscosity as compared to other cutting fluids. The addition of Al_2O_3 NPs in the SO+DW emulsion increased viscosity. Increasing the concentration of Al_2O_3 NPs from 0.5 to 1 wt.% may result in the accumulation of NPs in the SO+DW. This can have an impact on the lubricant's ability to form a film. It was also observed from the study presented by Wang et al. [278] that the viscosity increased with an increase in the addition of Al_2O_3 NPs concentration (wt.%) in the pure palm oil as base fluid.

6.1.7 Surface tension of cutting fluid

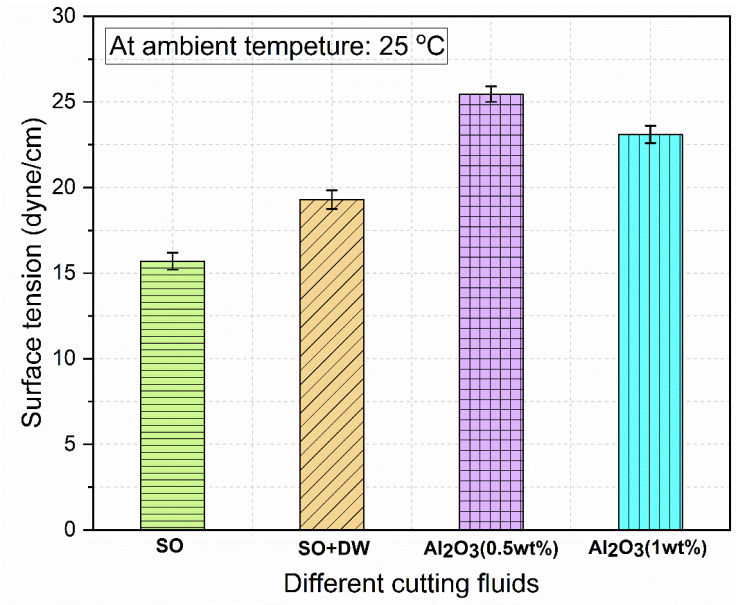

Figure 6.9 Surface tension of different cutting fluids

Surface tension plays a crucial role in the formation and stability of emulsions and nanofluids. An emulsion is a mixture of two immiscible liquids, such as oil and water, stabilized by a third substance known as an emulsifier. The emulsifier works by reducing

the interfacial tension between the two liquids, allowing them to mix and form a stable emulsion. Similarly, in nanofluids, which are suspensions of nanoparticles in a base fluid, surface tension helps to prevent the nanoparticles from agglomerating and settling out by creating a repulsive force between them. This repulsion is due to the reduction in the interfacial tension between the nanoparticles and the base fluid, which allows them to remain suspended for extended periods. According to Figure 6.9, due to intermolecular repulsive forces between the Al_2O_3 NPs, the surface tension decreased as their concentration in the emulsion increased. This happens because nanoparticles can adsorb onto the interface between the two liquids and create a repulsive force that opposes the cohesive forces of the liquids. As reported in a recent investigation, the presence of a long-chain surfactant in nanofluids led to the creation of a monolayer, which resulted in stronger electrostatic repulsive forces between Al_2O_3 NPs [270]. The pendant drop method was used to measure the surface tension of SO, SO+DW emulsion, and nanofluids with different concentrations, as discussed in Chapter 3, section 3.7. Therefore, surface tension values were obtained in increasing order for SO, SO+DW emulsion, Al_2O_3 NFs (1 wt.%), and Al_2O_3 NFs (0.5 wt.%), as depicted in Figure 6.9. SO+DW emulsions significantly increased surface tension compared to pure vegetable oil (SO) because of the presence of two hydrogen (H) and one oxygen (O) atom in deionized water, making a strong link between them.

6.1.8 Wettability of cutting fluid with AISI D2 tool steel

Wettability is an important thermo-physical property that determines the extent to which a liquid can spread over a solid surface using a Drop Shape Analyzer system (refer to Figure 3.9 (b)). The wettability of a surface can be characterized by the contact angle formed through the liquid droplet on the surface, as seen in Figure 6.10. When a liquid droplet comes into contact with a solid surface, an angle is produced between the tangent of the

droplet and the surface. This angle is referred to as the contact angle. In most applications, the air was always considered as the III phase. The workpiece and liquid droplet were considered as phases I and II, respectively (refer to Figure 6.10). Generally, the evaluation of the theory of surface tension may clarify the contact angle theory. The surface tension of three distinct interfaces were assessed as solid-air ($\mu_{s.a}$), solid-liquid ($\mu_{l.s}$), and liquid-air ($\mu_{l.a}$), respectively. The relationship between the equilibrium contact angle (θ) and the surface tension of various phases is represented by Thomas Young's equation [279]. A mathematical expression is given by the equation (6.1):

$$\cos\theta = \left(\frac{\mu_{s.a} - \mu_{l.s}}{\mu_{l.a}}\right) \tag{6.1}$$

This model assumed that the size of the liquid droplet was small so that gravity could be negligible. For contact angle measurements, the surface of the solid substrate must be flat and homogenous. The surface's wetting property is described as follows: if the θ is less than 90°, the material's behaviour is hydrophilic, increasing the wetting area; if the θ is more than 90°, the material's behaviour is hydrophobic, resulting in less wetting area.

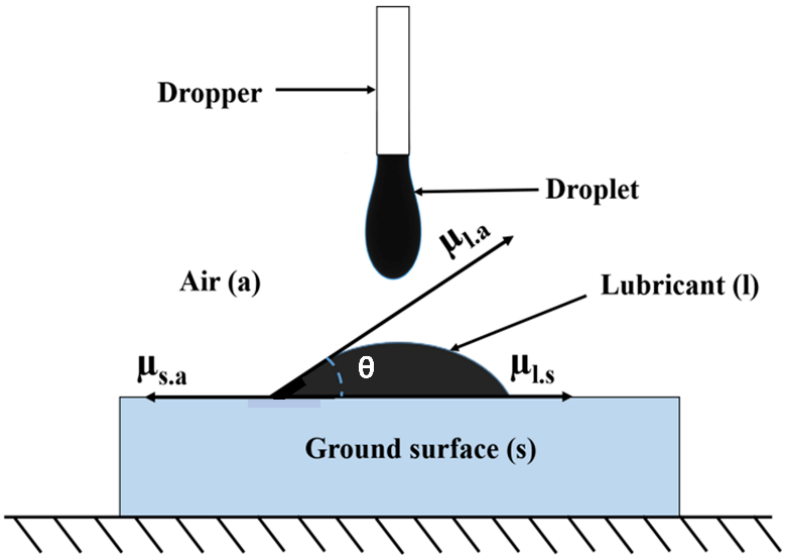

Figure 6.10 Schematic of cutting fluid droplet on the ground surface

Figure 6.11 shows a pictorial view of the Drop Shape Analyzer for wettability analysis and depicts the contact angle values for SO, SO+DW, and nanofluids at different NPs concentrations ranging from 0.5 to 1 wt.%. A sessile drop method was utilised to determine the contact angles of various cutting fluids. Before the wettability test, acetone was used to clean the ground surface. Further, lubricant through a dropper was dropped on the ground surface. The lubricant droplet image was captured and noted the contact angle value. In the case of soybean oil as shown in Figure 6.11 (a), the contact angle was recorded (30.5°). The reason is the higher viscosity of soybean oil (refer to Table 6.2 and Figure 6.8), which resists the oil flow rate over the ground surface during grinding.

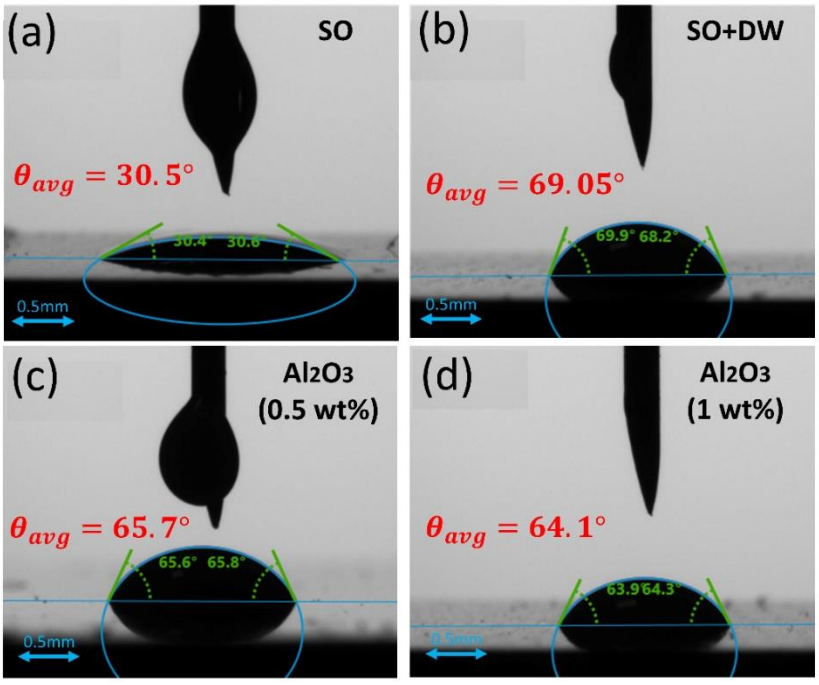

Figure 6.11 Contact angle of different cutting fluids with AISI D2 tool steel ground sample

This resulted in the poor wettability of soybean oil. According to Mishra et al. [32], oil viscosity is inversely proportional to the flowability or penetration of oil. On the other hand, higher viscosity helps to create a strong lubricating film on the ground surface.

Correspondingly, friction coefficient and surface roughness were reduced, drastically improving ground surface quality.

In the case of nanofluids, a low contact angle was observed on the ground workpiece, followed by oil-water emulsion. Adding Al_2O_3 NPs in emulsion (SO+DW) indicated a lower contact angle. In Figure 6.11 (b-d), it was observed that Al_2O_3 NFs with 1 wt.% concentration exhibited a minimum contact angle, indicating a higher wetting ability on the surface than the emulsion and Al_2O_3 NFs (0.5 wt.%). The reason is that Al_2O_3 NPs show higher order of magnitude in terms of size and density, thus enabling the exertion of additional downward extrusion force on oil-water emulsion along the contact surface.

6.2 Results and discussion

An experimental investigation was carried out to compare the surface grinding performance of work material under two distinct environments, namely MQL and UVAMQL. These environments included four lubricants, i.e., SO as base fluid, SO+DW emulsion, 0.5 wt.% Al_2O_3 NFs, and 1 wt.% Al_2O_3 NFs. This study presented the investigation results of various response characterises related to the grinding process, including grinding force, surface roughness, surface functional parameters, ground surface topography, chip morphology, and grinding temperature in subsequent subsections.

6.2.1 Grinding force

In the grinding process, grinding force is an essential technical parameter. This parameter relates to the service life of the grinding wheel and surface roughness. It is described as the force needed to remove material during grinding. However, it also reflects the lubrication performance of various grinding fluids used during the grinding operation. Figure 6.12 shows the grinding force of the different cutting fluids under MQL and UVAMQL grinding modes. Grinding force is divided into tangential force (F_t) and normal force (F_n) for

analysis. The trend of grinding force (F_t and F_n) for four different cutting fluids in MQL and UVAMQL grinding measured by a dynamometer is shown in Figure 6.12. The grinding force was found to be in the order of low to high as UVAMQL < MQL grinding mode, and the grinding force of the cutting fluids in MQL and UVAMQL grinding mode appeared by order of SO+DW > Al_2O_3 (0.5wt.%) > SO > Al_2O_3 (1 wt.%). The excessive negative rake angle of unidirectional rotation alumina grits and the high apparent friction coefficient of the grit-work-chip interface cause the highest grinding force in SO+DW emulsion. Additionally, Al_2O_3 NPs can help to reduce friction at the abrasive wheel and the workpiece interface, resulting in reduced grinding forces and improved surface quality [118].

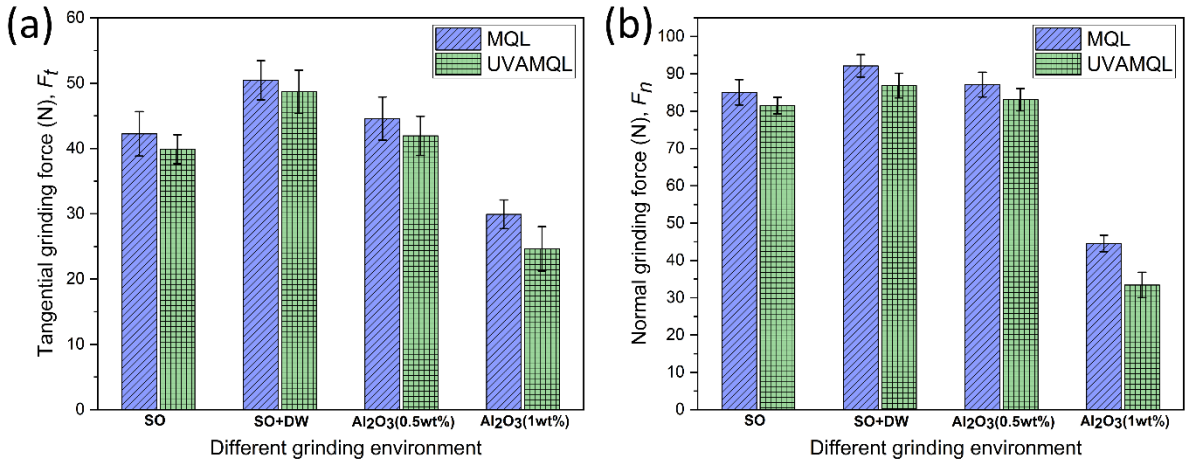

Figure 6.12 Grinding forces (a) F_t, (b) F_n under MQL and UVAMQL grinding with different cutting fluids

However, for grinding in the UVAMQL mode, the F_t for SO, SO+DW, Al_2O_3 (0.5 wt.%), and Al_2O_3 (1 wt.%) was reduced by 5.56%, 7.36%, 9.39% and 21.66%, respectively, over MQL grinding at the wheel speed of 39.42 m/s and downfeed of 40μm. Similarly, the F_n was lowered by 6.52%, 7.71%, 8.40% and 26.67%, respectively, over MQL grinding.

The UVAMQL grinding mode is more efficient than MQL grinding mode because, in the case of UVAMQL grinding, a minimum quantity of lubricant is used along with ultrasonic vibrations. The lubricant acts as a coolant, reducing friction between the grinding wheel

and the workpiece. The ultrasonic vibrations help to distribute the lubricant more effectively by inducing cavitation and improving its penetration into the grinding zone. Improved lubrication reduces the generation of heat and friction, resulting in lower grinding forces. Furthermore, the ultrasonic vibrations create oscillations in the workpiece, resulting in micro-level motion at the contact interface. This motion helps to disrupt the formation of strong adhesive bonds between the grinding wheel and the workpiece, reducing friction [192]. Lower friction means less resistance during grinding, leading to lower grinding forces. With the introduction of NPs, the Al_2O_3 NPs (1 wt.%) have the lowest grinding force compared to other lubricants under MQL and UVAMQL grinding mode. It happens due to the unique properties of Al_2O_3 NPs (1 wt.%), such as high thermal conductivity and low contact angle, which enable enhanced heat dissipation and lubrication effect [280].

6.2.2 Surface Roughness

Surface roughness refers to the irregularities and variations in a workpiece's surface texture. The Mitutoyo roughness tester measures the surface roughness on the ground surface produced by randomly distributed abrasive grains. The decreased surface roughness enhances the ground sample's physical, mechanical, and tribological qualities. Several standard roughness parameters, i.e., R_a, R_q, and R_z, describe quantitative information of surface quality. Generally, surface roughness is influenced by the wheel wear rate, adhesion of microchips and grits, and

lubricating conditions during the grinding [105]. Figure 6.13 demonstrates that R_a, R_q, and R_z display similar trends for all investigated conditions. In the case of UVAMQL grinding mode the surface roughness was reduced by 17.61%, 7.77%, 14.78%, 21.56% in R_a parameter, 16.19%, 11.81%, 15.84%, 17.42% in R_q parameter, and 8.23%, 23.28%, 15.97%, 14.52% in R_z parameter compared to the SO, SO+DW, Al_2O_3 (0.5wt.%) NFs, and Al_2O_3 (1 wt.%) NFs in MQL grinding mode, respectively.

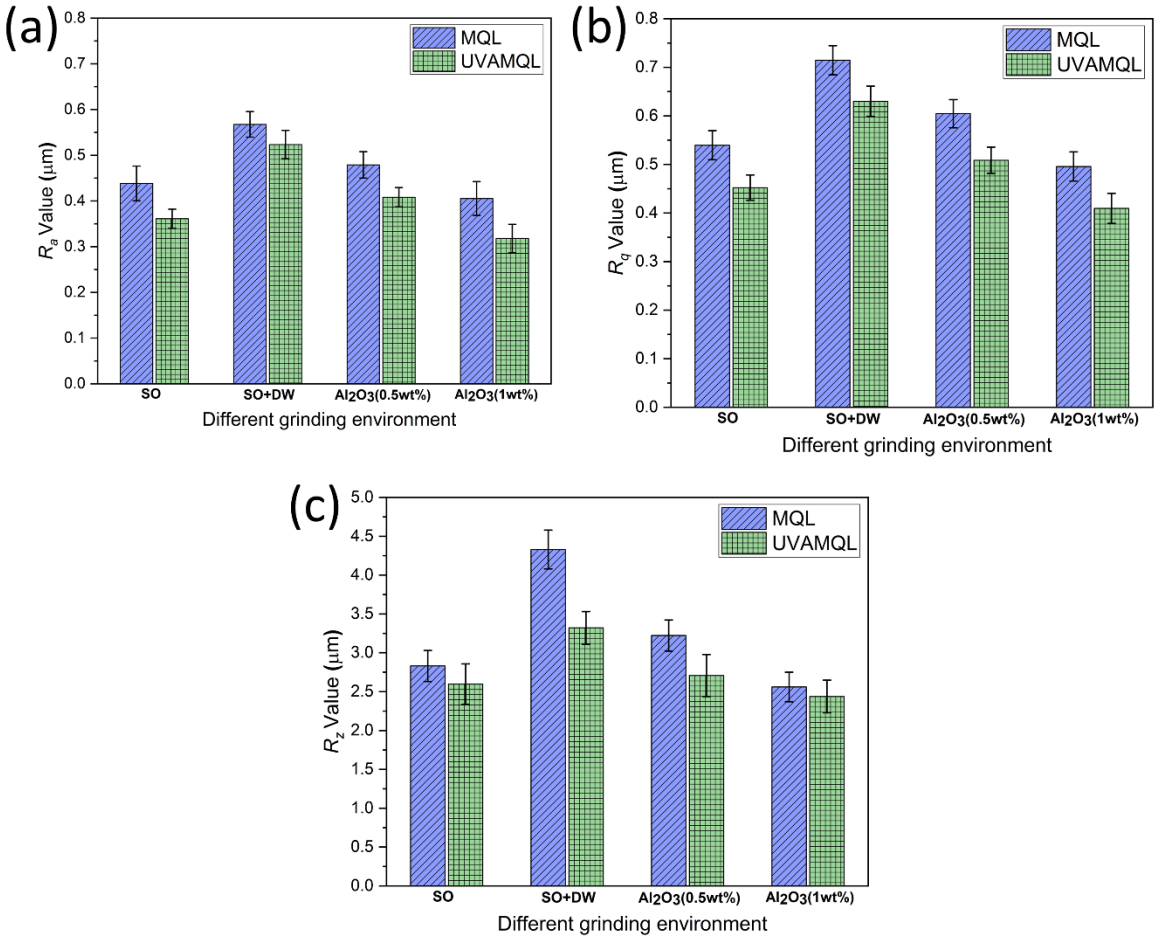

Figure 6.13 Surface roughness (a) R_a, (b) R_q, (c) R_z under MQL and UVAMQL grinding with different cutting fluids

The R_a, R_q, and R_z results showed that the best surface roughness is achieved under the UVAMQL grinding mode using Al_2O_3 (1 wt.%) NFs with R_a of 0.3179 μm, R_q of 0.4094 and R_z of 2.43 μm. For this reason, the Al_2O_3 NPs can also help to disperse heat generated from the grinding zone area, which can reduce the risk of thermal damage to the work material. Furthermore, Al_2O_3 NPs can act as a filler, filling in microcracks and other imperfections in the workpiece surface. This can result in a smoother and more uniform surface finish. Similar results were obtained by previous researchers [193], They added Al_2O_3 NPs of 40 nm average size with different volumetric concentrations in water as the grinding fluid and sprayed Al_2O_3 NFs on hardened AISI52100 steel during the ultrasonic vibration assisted MQL grinding experiment. A better surface finish was observed over the

ground surface by Al_2O_3 NPs than coolant and pure water, and the grinding force was significantly reduced. Also, the NPs with ultrasonic vibration may sharpen the abrasive wheel during the grinding process, and UVAMQL grinding with nanofluid significantly improves surface roughness. It was reported by Molaie et al. [118] that the improvement in the surface roughness under UVAMQL grinding mode was because of the grit motion with low friction in horizontal vibration creates a higher chance of cutting the peaks of the surface. Additionally, as ultrasonic vibration assisted grinding utilizes supplementary stress to support in disintegrating the instantaneous welds, they decrease the time in the course of which any two asperities on counter surfaces may continue in temporary contact and, therefore, it prevents them from developing a stable weld [90]. This implies that in UVAMQL grinding, a lesser amount of stable bonds among the abrasive grits and workpiece material surface is formed, and with eco-friendly cutting fluids cooling and lubrication occur more efficiently. Hence the surface roughness decreases more in UVAMQL grinding mode than in MQL grinding mode.

6.2.3 Surface functional parameters

According to the EUR 15178N standards for evaluating the surface functional parameters such as surface bearing index (*Sbi*) and core fluid retention index (*Sci*) introduced by Dong et al. [281], the surface frictional characteristics of the finished component were examined. The following is the definition and mathematical formulation of the functional parameters as described by:

$$Sbi = \frac{S_q}{\eta_{0.05}} \tag{6.2}$$

The *Sbi*, which evaluates the load-bearing capability of a workpiece surface, is known as the ratio of the root mean square deviation over the surface height at a five-percent bearing area [281].

The *Sci* is described as the ratio of void volume per unit sampling area at the core zone to root mean square deviation. It represents the capability of a surface of the workpiece to maintain lubrication in the surface's core zone [281].

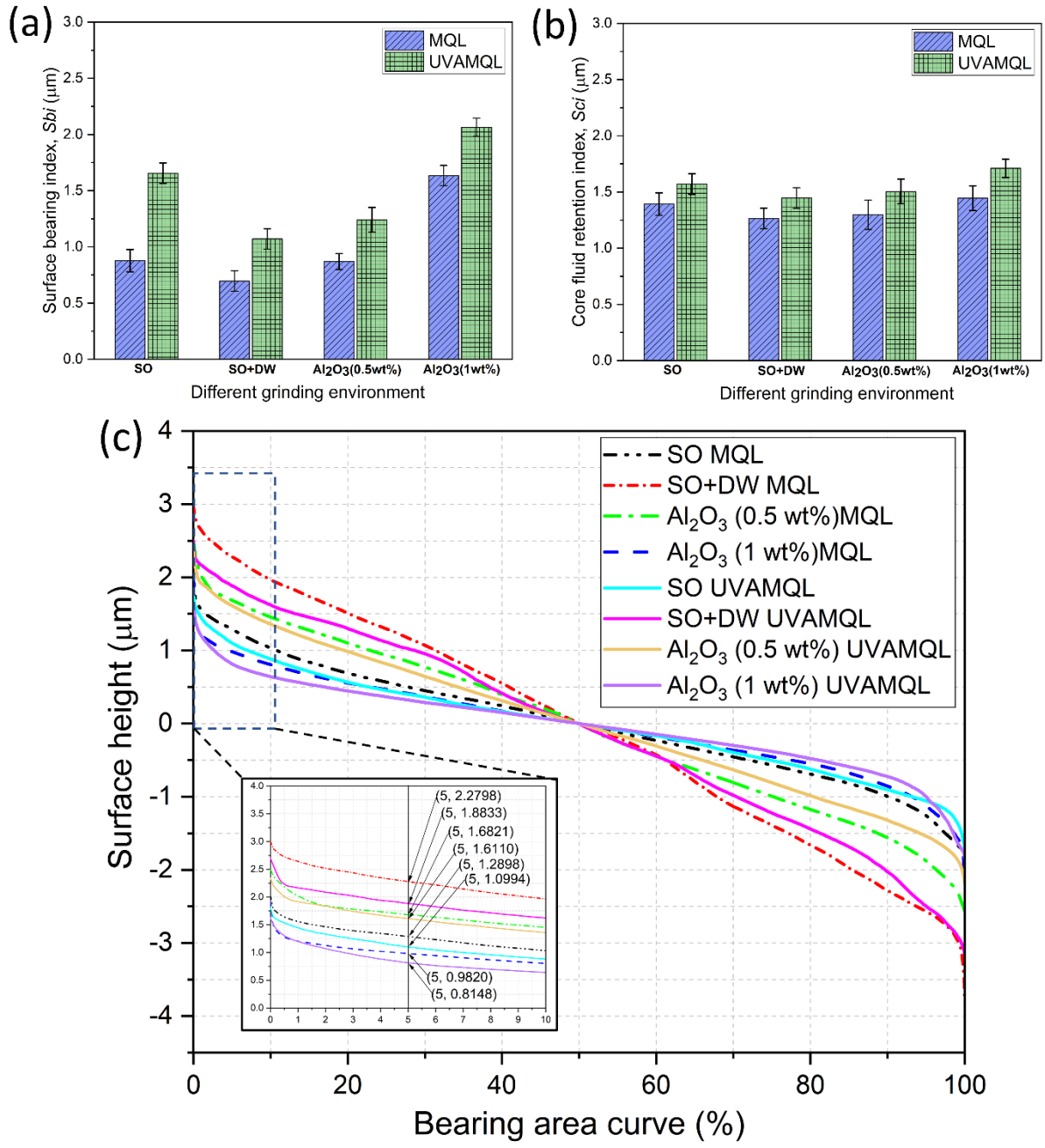

Figure 6.14 Variation in surface functional parameters under various modes, (a) *Sbi*, (b) *Sci*, (c) bearing area curve

$$Sci = \frac{1}{S_q} \frac{V_v(h_{0.05}) - V_v(h_{0.08})}{(M-1)(N-1)\Delta x \Delta y} \quad (6.3)$$

Where S_q is the root mean square deviation; $\eta_{0.05}$ is the surface height at a five-percent bearing area; $V_v(h_{0.05})$ and $V_v(h_{0.08})$ are the void volumes of the surface heights $h_{0.05}$ and $h_{0.08}$; *M* and *N* are the numbers of sample points in the *x* and *y* directions; Δx and Δy are the samplings periods [281].

The effect of different eco-friendly cutting fluids on the *Sbi* and *Sci* under MQL and UVAMQL grinding modes are experimentally analysed by the AFM instrument, and the change trends of the surface functional parameters are illustrated in Figure 6.14 (a-c). In the case of UVAMQL grinding mode, the value of *Sbi* is maximum in Al_2O_3 (1 wt.%) NFs, and minimum in SO+DW emulsion as shown in Figure 6.14 (a). This is most likely caused by the *Sbi*, which is stated in Equation (6.2) to be proportional to surface roughness S_q and inversely proportional to surface heights at a five percent bearing area $\eta_{0.05}$. The experimental surface roughness S_q typically highest in case of SO+DW and lowest in case of Al_2O_3 (1 wt.%) NFs under both grinding modes, as shown in Figure 6.16, and the correlation between the height distribution and the topographical feature is $\eta_{0.05}$. The variations in the height distribution and topographical features are typically minimal for the same processing method. Because of its proportionate correlation with the S_q, the *Sbi* under this investigation could consequently increase. The load-bearing capability of the UVAMQL ground surface is observed to be significantly higher than that of the MQL ground surfaces under each cutting fluids respectively, regardless of the alikeness in the rising tendency of the *Sbi* graphs in all modes of grinding. The enhanced surface quality caused by the discontinuous interaction between the abrasive wheel and workpiece along with more efficient cooling and lubrication using different eco-friendly cutting fluids, which can considerably reduce the influences of the thermal damage, rubbing and plowing

marks on the ground surface, may also be attributed to the more significant value of the *Sbi* in the UVAMQL grinding mode. This suggests UVAMQL grinding mode's surface has an improved bearing characteristic in all the case compared to MQL grinding mode. Figure 6.14 (b) represents how the different cutting fluids affects the *Sci*, and it can be seen that the *Sci* exhibits higher values under UVAMQL grinding mode compared to MQL grinding mode. This may be because the relation between the *Sci* and S_q is inversely proportional. The corresponding height factor derived from Equation (6.3) may also be used to explain the observed influence. As was previously noted, the S_q value highest in SO+DW and lowest in the Al_2O_3 (1 wt.%) NFs in both mode of grinding. According to Dong et al. [281], the higher *Sci* showed an improved fluid retention property in the core region. This shows that the lubrication oil contained in the groove will perform effectively in lubricating the friction parts on the ground surface generated by the UVAMQL grinding mode. As illustrated in Figure 6.14 (a-b), the *Sbi* and *Sci* are higher in UVAMQL mode. The principal cause of this observations is that the ultrasonic vibration alters each abrasive grit track. A sine waveform governs the UVAMQL grinding track; its length would be greater than an MQL grinding mode (refer to Figure 1.6 (b)). Denoting that the abrasive grits in UVAMQL grinding mode would interact with one another and cause larger overlapping of the material removal compared to that of MQL grinding mode. Therefore, fewer grinding marks and a smooth workpiece surface finish would have been obtained. Figure 6.14 (c) represents the surface height at the five bearing areas for the MQL and UVAMQL grinding modes with SO, SO+DW, Al_2O_3 (0.5wt.%) NFs, and Al_2O_3 (1 wt.%) NFs in order to better comprehend the effect of the topographical characteristic on $\eta_{0.05}$. The surface height at the five percent bearing area for SO, SO+DW, Al_2O_3 (0.5wt.%) NFs, and Al_2O_3 (1 wt.%) NFs under MQL grinding mode are 1.2898µm, 2.2798µm, 1.6821µm, and 0.9820µm, which is significantly greater as compared to UVAMQL grinding mode, i.e., 1.0994µm,

1.8833μm, 1.6110μm, and, 0.8148μm, respectively, as shown in Figure 6.14 (c). It may be owing to the comparatively flat top surface's bearing area ratio rising rapidly from zero bearing to five percent. This results in a decrease in *Sbi* in MQL grinding mode. In addition, the topographical characteristic is associated with the impact of overlapping induced through ultrasonic vibration along with Al_2O_3 (1 wt.%) NFs may result in a more pronounced effect of overlapping. This may explain how $\eta_{0.05}$ reduces when the UVAMQL grinding with Al_2O_3 (1 wt.%) NFs, leading to a rise in *Sbi*. A specific quantity of energy is needed for the grinding operations to ground the workpiece, and the majority of this energy is transformed into heat. Thus, heat is transferred into the workpiece, leading to thermal damage, and subsequently diminishing the workpiece's operational life [282]. The surface generated by the UVAMQL grinding mode with Al_2O_3 (1 wt.%) NFs (refer to Figure 6.15 (h)) is clearly finer and gives greater bearing characteristics, which is critical in frictional applications.

6.2.4 Ground surface topography

Surface topography is a crucial evaluation index that helps determine the surface integrity of machined specimens. When it comes to directly evaluating the surface integrity of ground samples, the scanning electron microscope (SEM) and the atomic force microscope (AFM) are generally considered to be the most effective methods. Figure 6.15 illustrates the changes in the surface characteristics of the ground surface with different cutting fluids under MQL and UVAMQL grinding modes. In the MQL technique, the insufficient absorption ability of the lubricating film of the SO + DW emulsion has led to the microchip sticking to the entire ground surface, causing noticeable side flows, deep groove, and redeposited materials. Due to the low thermal conductivity and viscosity of SO + DW emulsion (refer to Figure 6.7 and Figure 6.8), the grinding zone area experienced a higher temperature than other cutting fluids. This can cause the major portion of grinding chips on

the alumina wheel to become smeared or loaded, further redeposited over the ground surface. Large numbers of uneven abrasive grits distributed discretely composed the grinding wheel surface. As a result, deep scratches and grooves were produced on the ground surface along the grinding marks direction, and also side flows by the ploughing action of abrasive grits were found, as shown in Figure 6.15 (c). A nearly good surface texture was achieved in UVAMQL grinding mode using SO+DW emulsion (refer to Figure 6.15 (d)) compared to MQL grinding mode under same condition. The reason for this is attributed to uniformly distribution of the SO+DW emulsion on the workpiece surface with the help of ultrasonic vibration during UVAMQL grinding. This helps in reducing the plowing, rubbing and promoting the shearing action by sharp abrasive grits. A thick adsorption film layer on the ground surface due to higher viscosity (refer to Table 6.2) and effective molecular structure of SO (refer to Figure 6.1(b)), which in turn enhances the slipping action of the abrasive grits over the ground surface. This led to minimum grooves and scratches the ground surface using SO during MQL and UVAMQL grinding modes, as shown in Figure 6.15 (a-b).

Application of Al_2O_3 NFs in MQL and UVAMQL grinding modes resulted in a better surface morphology than SO and SO+DW cutting fluids under MQL and UVAMQL grinding modes, respectively. This improvement suggests that the presence of Al_2O_3 NPs helps to reduce adhesion between the abrasive grain and workpiece by providing adequate lubrication through rolling and sliding phenomena and uniform cooling through mass heat transfer from the grinding zone, which consequently lowers the grinding force and friction [283]. On the other hand, Figure 6.15 (h) shows a better surface texture in comparison to all the cutting fluids owing to the higher concentration of Al_2O_3 (1 wt.%) NPs, and ultrasonic vibration helps to enhance cooling and lubrication under the UVAMQL grinding modes.

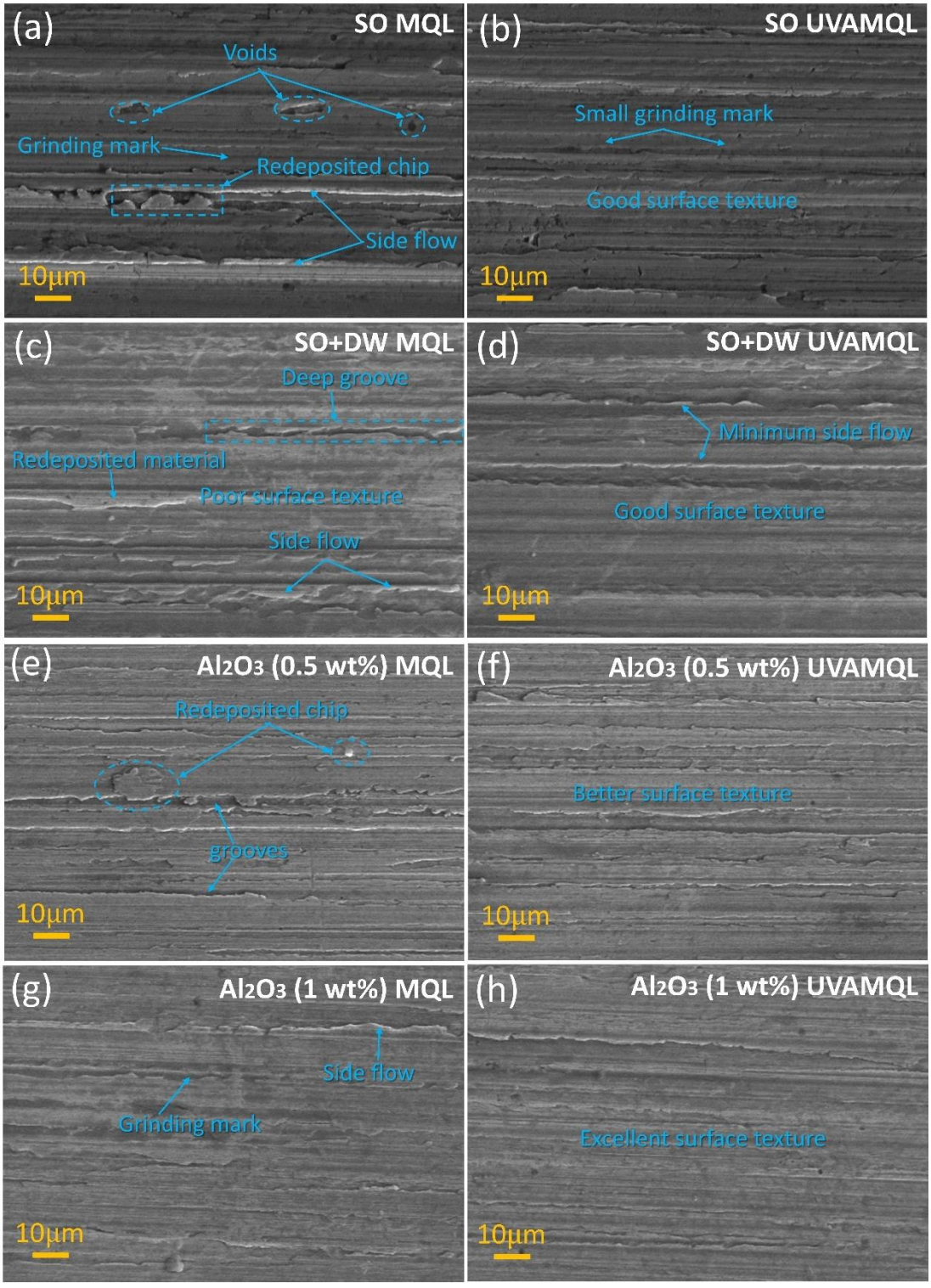

Figure 6.15 Surface morphology of work material under MQL and UVAMQL grinding modes

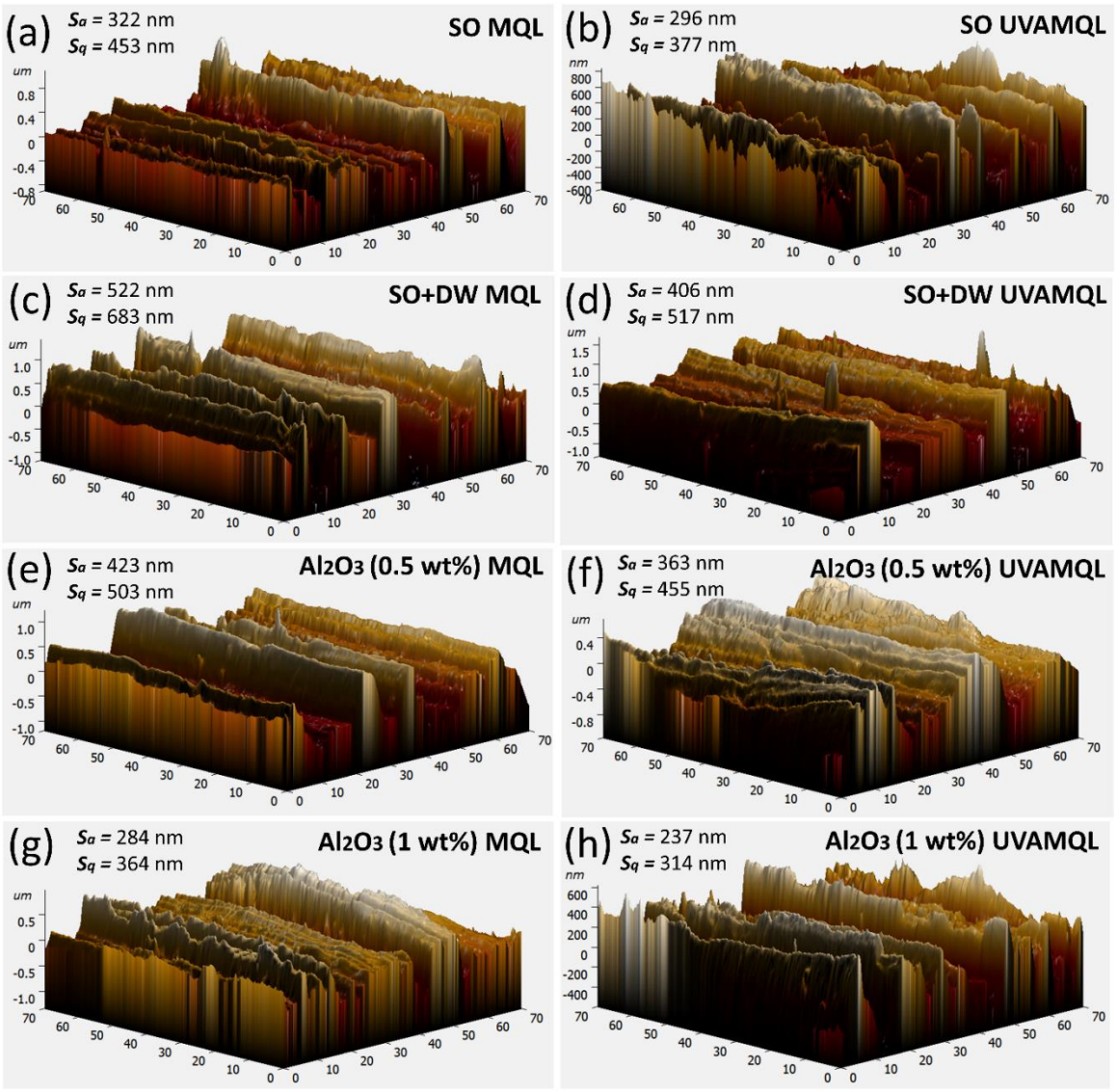

Figure 6.16 3D surface topography of AISI D2 tool steel under MQL and UVAMQL grinding modes

Three-dimensional surface topography provides a more accurate and detailed representation of the physical features of the ground surface. Because 3D topography allows for the identification and analysis of topographical features, such as peaks and valleys heights, that may not be apparent in 2D morphology. Figure 6.16 depicts 3D surface topography images obtained using AFM instruments operating under MQL and UVAMQL grinding modes. AFM analysis obtained the most optimal surface roughness measurements for a ground sample with 1 wt.% Al_2O_3 NFs-based UVAMQL grinding mode. This method

provided the superior impact of cooling and lubrication, resulting in a small average roughness (S_a: 237 nm) and low root mean square roughness (S_q: 314 nm), an illustrated in Figure 6.16 (h). In addition to that in all the cases of MQL grinding mode, the ground surface described by typical peaks and valleys comprises deep and narrow linear grooves, and the ground surface quality is certainly less desirable than that in UVAMQL grinding mode. However, the grinding grooves in UVAMQL grinding mode are not as straight as those in MQL grinding mode, and intermittent relatively flat peaks can be observed. As a result, the surface roughness in all the cases of UVAMQL grinding mode decreases, respectively.

6.2.5 Grinding microchip morphology

Chip morphology is essential for the grindability of the work material. Grinding microchip morphology, size, and shapes are significantly impacted by the combined influences of the mechanical properties of the work material and the abrasive wheel, as well as the grinding parameters, particularly the grinding mode, downfeed, table feed rate, and wheel speed. Figure 6.17 (a-h) shows the morphology of grinding microchips collected on carbon tape upon different eco-friendly cutting fluids under MQL and UVAMQL grinding modes. AISI D2 tool steel has poor heat transfer capability owing to its thermo-mechanical properties. Therefore, a large amount of heat accumulated on the ground surface, and the sample got thermoplastic unbalance conditions. Generally, thermal expansion and contraction of finished samples occur due to huge heat generation. The surface of the workpiece extends as the abrasive wheel goes over it. The surface rapidly cools once the wheel has passed, and the ground sample quenches it. This resulted in micro-cracks and residual stress formation in the ground surface and subsurface. This happens due to the thermoplastic unbalance condition of the ground sample at higher temperatures. Microchips were formed in curl or spiral shape under extruding shearing action and thermal gradient issue [116].

Thus, long continuous ribbon types of chips were formed during SO as base fluid and SO+DW emulsion under MQL grinding, as shown in Figure 6.17 (a and c). It happened because of the low thermal conductivity in comparison to the Al_2O_3 NFs. When Al_2O_3 NPs are added to the vegetable oil-based deionized water emulsion used in MQL grinding, they can form a lubrication boundary layer at the grinding zone, reducing friction at the wheel-workpiece interface and grinding force. This, in turn, reduces the temperature generated during the machining process and increases the proportion of small chips while reducing the proportion of long chips. During the UVAMQL grinding, C-type chips, small discontinuous chips, fragmented chips, shear chips, and flow chips were observed as the temperature decreased and the grinding force by the combined effect of ultrasonic vibration and eco-friendly cutting fluids. This phenomenon can be attributed to the cutting track alteration and a split-up stage between the abrasive grit particles and the workpiece. In UVAMQL grinding mode, the matching long continuous grinding chips were split into short discontinuous grinding chips with thinner, short morphologies. Besides, fragmented chips were easier to handle than long chips, and they could not adhere to the surface, leading to better surface quality. Moreover, such chips could be disposed of with significantly low hassles. In particular ways, the separating characteristics of UVAMQL grinding mode enable chip breakdown. However, based on the results shown in Figure 6.17 (h), it can be inferred that utilising ultrasonic vibration with Al_2O_3 NPs (1 wt.%) concentration improved chip breakability, thus suggesting the superior grindability performance of AISI D2 tool steel.

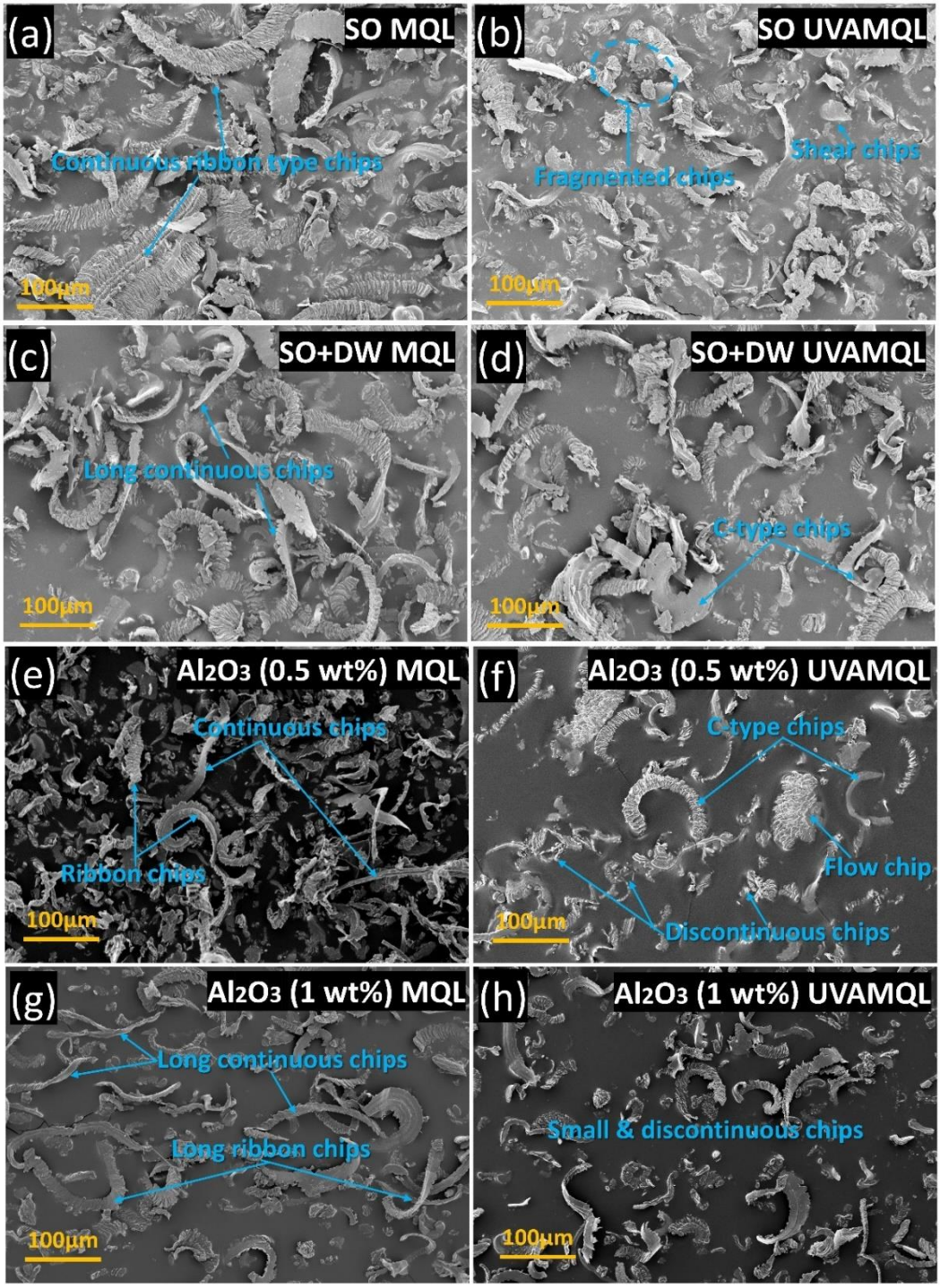

Figure 6.17 SEM micrograph of microchip under MQL and UVAMQL grinding modes with different eco-friendly cutting fluids

6.2.6 Grinding temperature

The grinding temperature has a significant impact on the grinding process. It changes the physical properties of the workpiece and the grinding wheel, affecting the material removal

rate, surface quality, and overall efficiency of the grinding operation. During the grinding process, friction between the abrasive wheel and workpiece produces heat that leads to wear and tear of the abrasive wheel and deteriorates the workpiece's surface quality in terms of poor surface finish. Hence, analysing the grinding temperature produced during grinding AISI D2 tool steel is essential. The expression of the average total heat flux (Q) in the contact zone during the grinding process can be described as [8].

$$Q = \frac{F_t \times V_c}{W \times l_c} \tag{6.4}$$

Where F_t is tangential grinding force, V_c is wheel speed, W is the width of the workpiece, and l_c is the length of contact of the abrasive wheel with the workpiece. As the tangential grinding force decreases, the heat flux and maximum grinding temperature decrease, as stated by this equation (6.4). In this analysis, the temperature was recorded by a high-speed infrared thermographic camera. Figure 6.18 (a-h) illustrates the maximum grinding temperature under MQL and UVAMQL grinding modes with four eco-friendly cutting fluids. As shown in Figure 6.18 (a-h), UVAMQL grinding mode has a lower grinding temperature compared to MQL grinding mode with corresponding eco-friendly cutting fluids, respectively. This is due to the lower tangential grinding force obtained in UVAMQL grinding mode (refer to Figure 6.12 (a)), resulting in the decrease of heat flux and grinding temperature in the grinding zone (refer to equation 6.4). As discussed earlier, less thermal conductivity produces maximum heat under SO-based grinding, causing more wheel wear and poor surface integrity than other cutting fluids. Compared to SO-based grinding, the temperature was lower when a SO+DW emulsion was sprayed in the grinding zone.

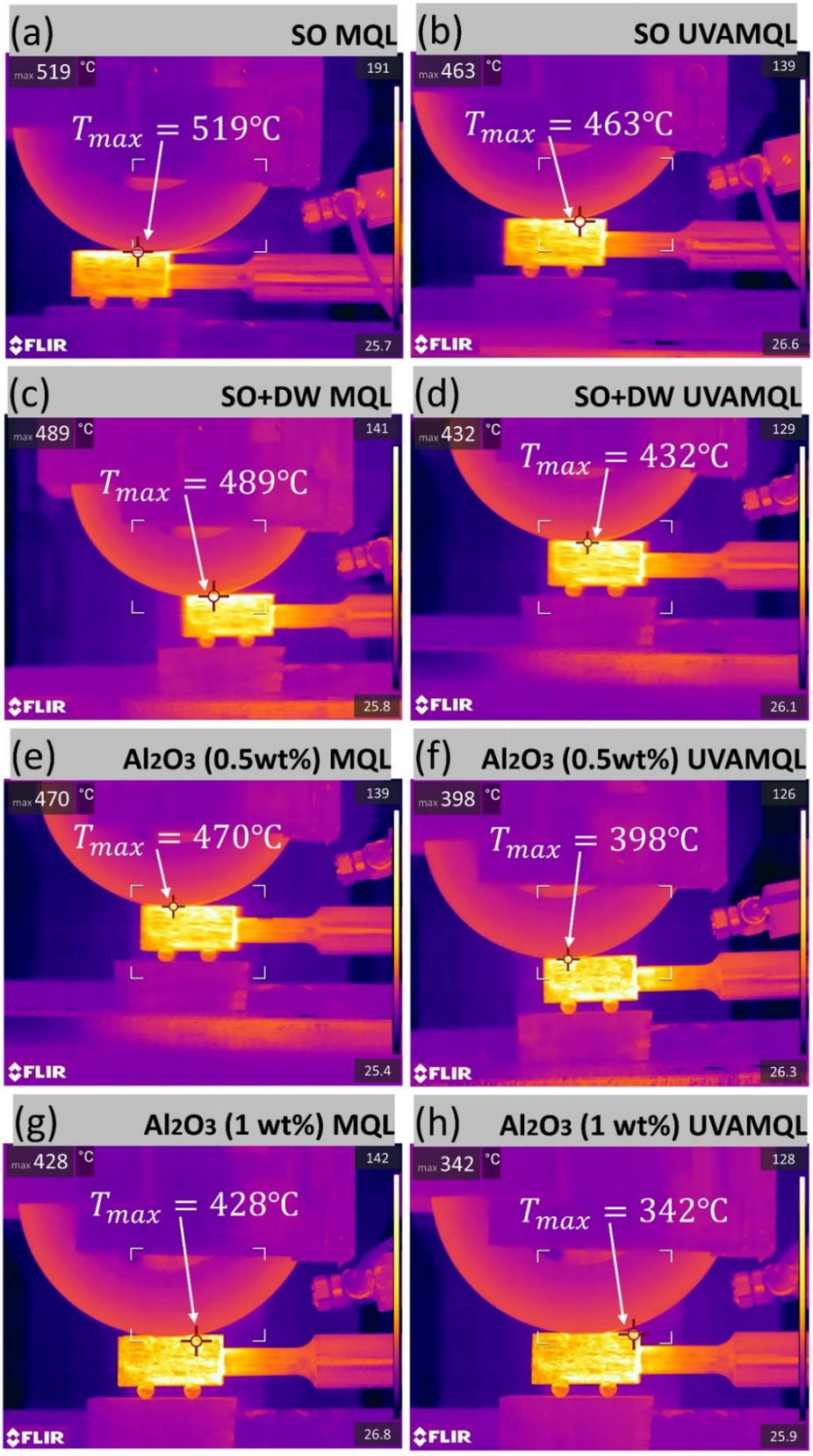

Figure 6.18 Infrared thermographic grinding temperature profile under MQL and UVAMQL grinding modes with different eco-friendly cutting fluids

Compared to SO and SO+DW grinding, Al_2O_3 NPs significantly reduced grinding temperature. The lowering in grinding temperature with Al_2O_3 NFs is due to the higher thermal conductivity (refer to Figure 6.7). This is because nanofluid has better lubrication properties, enhancing the tribological properties between the grinding wheel and workpiece interfaces and retaining the abrasive grains for an extended period. The lowest grinding temperature was recorded in UVAMQL grinding mode using Al_2O_3 (1wt.%) NFs, as shown in Figure 6.18 (h). The UVAMQL grinding mode decreases heat generated in the grinding zone by decreasing contact time between the abrasive grit and the workpiece.

Equations (6.5) and (6.6) can be used to determine the contact length (l_c) and cutting time (t_c) of a single abrasive grit in a surface grinding process.

$$l_c = \sqrt{D \times a_p} \tag{6.5}$$

$$t_c = \frac{l_c}{V_C} \tag{6.6}$$

Where D is the grinding wheel diameter, a_p is downfeed. In this analysis, the contact length and the cutting time are 3.16 mm and 8.1×10^{-5} s, respectively, for MQL grinding mode at a_p = 40 μm. However, the cutting time in UVAMQL grinding is not equal to that in MQL grinding. The period of ultrasonic vibrations is the reciprocate of the frequency, and as the f_{ug} = 21 kHz, the duration of each vibration cycle is 4.7×10^{-5} s. Therefore, in UVAMQL grinding mode, the cutting time will be shorter than that in MQL grinding mode, and due to Equation (6.6), the cutting speed in both grinding modes is equal, and the contact length in UVAMQL grinding mode is reduced to 1.8 mm. As a result of the decrease in the contact length in UVAMQL grinding mode, grinding zone temperature and cutting forces are lowered.

On the contrary, discontinuous cutting action/workpiece separation provides a gap for dissipating heat between the cutting edge and the workpiece. So, more efficient cooling and

lubrication effects are achieved compared to the MQL grinding mode. Also, due to the lower rubbing and ploughing under UVAMQL grinding, the chance of thermal damage to the workpiece surface can be less.

6.3 Conclusion

A green hybrid UVAMQL grinding technique has been introduced in this Chapter to enhance the grindability of work material in surface grinding operations based on lubrication and cooling performance. A comparison of UVAMQL grinding with MQL grinding at different eco-friendly cutting fluids, namely, base fluid (SO), emulsion (SO+DW), and Al_2O_3 NFs (0.5 and 1 wt.%), was made to investigate their grinding performance regarding grinding force, surface roughness, surface functional parameters, ground surface topography, chip morphology and grinding temperature. Also, thermo-physical properties of Al_2O_3 NFs with various weight concentrations were evaluated in terms of pH value, density, thermal conductivity, viscosity, surface tension, and wettability. Based on the analysis of the results obtained, the following conclusions can be drawn:

- Adding Al_2O_3 NPs in SO+DW emulsion has increased the pH value, density, thermal conductivity, and viscosity. But surface tension increased at a concentration of 0.5 wt.% of Al_2O_3 NPs, after which surface tension was slightly reduced. The investigation of wettability revealed a decrease in the contact angle of Al_2O_3 NFs with increasing concentration.
- Among all the respective eco-friendly cutting fluids, highly concentrated Al_2O_3 NFs are the most efficient cutting fluid for UVAMQL grinding since it generates the lowest grinding force (F_t: 24.64N and F_n: 33.41N) and surface roughness (R_a: 0.3179 µm, R_q: 0.4094 µm, and R_z: 2.43 µm).
- The *Sbi* and *Sci* values under UVAMQL grinding mode with Al_2O_3 NFs: 1 wt.% is higher than that under the remaining modes. The *Sbi* and *Sci* values show that the

UVAMQL grinding mode's ground surface has better bearing and fluid retention characteristics.

- SEM and AFM micrographs indicated that the deep grooves, metal side flow, and redeposited layer on the ground surface are minimum in the case of UVAMQL grinding mode. Besides, small, and discontinuous chip morphology in UVAMQL grinding mode compared to MQL grinding in all cases show the ease of grinding and the lesser force needed while grinding AISI D2 tool steel.
- The UVAMQL grinding mode, as compared to MQL grinding mode, produced a lower grinding temperature in all cases. This is due to the short contact time between the grinding wheel grits and workpiece and cools the grinding zone through convective heat transfer to the surrounding environment using eco-friendly cutting fluids.